IEICE TRANSACTIONS

on Electronics

VOL. E101-C NO. 12
DECEMBER 2018

A PUBLICATION OF THE ELECTRONICS SOCIETY

The Institute of Electronics, Information and Communication Engineers
Kikai-Shinko-Kaikan Bldg., 5-8, Shibakoen 3 chome, Minato-ku, TOKYO, 105-0011 JAPAN

PAPER

Extending Distributed-Based Transversal Filter Method to Spectral Amplitude Encoded CDMA

Jorge AGUILAR-TORRENTERA[†a)], ***Member***, **Gerardo GARCÍA-SÁNCHEZ**[†], **Ramón RODRÍGUEZ-CRUZ**[†], ***and*** **Izzat Z. DARWAZEH**[††], ***Nonmembers***

SUMMARY In this paper, the analog code modulation characteristics of distributed-based transversal filters (DTFs) suitable for use in spectrally encoded CDMA systems are presented. The DTF is verified as an appropriate method to use in high-speed CDMA systems as opposed to previously proposed methods, which are intended for Direct Sequence (DS) CDMA systems. The large degree of freedom of DTF design permits controlling the filter pulse response to generate well specified temporal phase-coded signals. A decoder structure that performs bipolar detection of user subbands giving rise to a Spectral-Amplitude Encoded CDMA system is considered. Practical implementations require truncating the spreading signals by a time window of duration equal to the span time of the tapped delay line. Filter functions are chosen to demodulate the matched channel and achieve improved user interference rejection avoiding the need for transversal filters featuring a large number of taps. As a proof-of-concept of the electronic SAE scheme, practical circuit designs are developed at low speeds (3-dB point at 1 GHz) demonstrating the viability of the proposal.

key words: *code division multiplexing, distributed amplifiers, high-speed electronics, modulation coding, optical receivers*

1. Introduction

Owing to its multiple benefits, Optical CDMA (OCDMA) is currently viewed as a promising technique to develop Multi-Gbit/s local area networks (LANs). Its ability to differentiate between users in the network is very attractive, as encoded signals conveying address information with no message overhead improve throughput, latency and network functionality. However, to realize its potential merits, each network node must be provided with high speed transmit and receive functions. Since the introduction of the OCDMA technique in the mid 80s, it was foreseen that the seamless processing of codes based on ultrafast optical devices would be the natural choice to access to substantial bandwidth of the optical fiber with minimal delay [1]. Although important advances in high-speed optical devices have been made, the current cost of providing optical signal processing at each network node is a key impediment in developing such networks on a wide scale. Moreover, developing OCDMA networks operating at hundreds of Gbit/s comes at higher cost compared to alternative multiplexing techniques over passive optical networks (PONs) such as wavelength division multiple access (WDMA) [2].

The term 'electronic processing of codes' was introduced in the context of electronic CDMA (ECDMA) for access networks on PONs as a low-cost alternative to optical processing [3]. The general concept of electronic processing of CDMA and other Spread Spectrum (SS) signals was first proposed and explored in 2002 [4] with design work elaborated in [5] and [6]. Several experiments have been reported in the literature from early developments based on Charge Transfer Devices (CTDs) working at moderate speeds (2 Gchip/s and 62.5 Mbit/s) [7] to prototyping transversal equalizers operated as data encoders and correlators at rate of 18 Gchip/s and 1.25 Gbit/s [8]. The fractionally-spaced equalizer, which is typically used to effect dispersion compensation in high speed fiber optic links [9], [10], were employed to encode data and despread Direct Sequence (DS) code-modulated pulses and transversal filter structures were used for group velocity dispersion compensation in [11].

Electronic circuits capable of working in the multi-Gbit/s regime requires transversal filters based on distributed principles as first proposed in [12] and demonstrated in 10 Gbit/s systems in [13]. With the advances in microwave active device technologies and the submillimeter control of transmission lines, monolithic microwave integrated circuits (MMICs) have been recognized as a viable technology to use in CDMA systems [5], [6]. The viability of the DTF to process CDMA signals was analyzed in [5], where it is shown that periodic correlations present zero intersymbol interference (ISI) in agreement with the signal design for optical systems in [14]. However, the utility of the filter method may be limited by the inability of DTFs to handle long sequences. High losses and rise time degradation constrain the number of distributed active cells to, typically, 7 or 8 taps [15], thus the length of sequences programmed in DTFs must be short. This shortcoming, together with the fact that multiple access interference (MAI) increases quickly as more pseudo-orthogonal users are added to the network, have significant negative impact on asynchronous operation. The technique therefore requires imposing synchronization to avoid excessive user interference. Potential solution for electronic processing with longer chip sequences were explored (by time shifting of two parallel DTF structures in [16]) and by using high-level modulation schemes in [17].

In this paper, the electronic processing of codes is ex-

Manuscript received March 13, 2018.
Manuscript revised August 8, 2018.

[†]The authors are with Universidad Autónoma de Nuevo León, FIME, 66450, México.
[††]The author is with University College London, United Kingdom.
a) E-mail: jorge.aguilart@uanl.mx

DOI: 10.1587/transele.E101.C.953

tended to an alternative method to encode and detect CDMA signals. A method for implementing spectral amplitude encoded CDMA (SAE-CDMA) systems based on the transversal filter is introduced. The new finite impulse responses (FIRs) of SAE-CDMA require distributed-based transversal filters to be designed with the highest number of degrees of freedom. This is based on filter structures featuring unequal interstage delays and unequal tap gains [12]. Each filter FIR is related (via the inverse Fourier transform) to a spectrum, which is shaped by assigning the phases of the available subbands to a pseudo-noise code. The resulting signals consist of several ultra-short pulses of larger amplitude variation than those of SS chip shape formats.

The electronic SAE-CDMA was introduced in [18] with the objective of developing a method to reduce user interference in ECDMA systems. The synthesis of filters implemented with predetermined spread-in-time signals was first suggested in [19]. However, in DTF design, the tapped delay line is highly constrained by bandwidth degradation of distributed structures and size limitations in MMIC implementations. Accordingly, it is necessary to truncate temporal phase-coded signals by a time window and equating the fundamental period of the signal to the filter span time. When dealing with spectrally encoded signals, the truncation in time poses a problem of interference appearing in the form of side lobes that spread over the available bandwidth. In SAE-CDMA systems, frequency overlapping introduces potentially substantial multi-user interference (MUI). In our electronic SAE decoder, the method to select phases of spread-in-time signals in [18] is considered as a viable alternative to demodulate matched and unmatched channels.

This works presents analysis based on experimental results of SAE systems. Since encoding and correlation depend heavily on the performance of distributed broadband circuits, experimental results of prototypes are necessary to make judicious design decisions and gain insight into implementation limitations. The accurate processing relies on achievable time and frequency responses of practical DTFs. This papers experimental work analyzes encoding and decoding in the form of transmission and reception of high-rate pulses with controlled interference. Also, distributed circuit design strategies are outlined to contrast with previous temporal encoding approaches.

The rest of the paper is organized as follows: Sect. 2 provides a brief description of optical SAE-CDMA systems, Sect. 3 shows the transversal filter topology suitable to develop a proof-of-concept of the proposed CDMA system. Section 4 shows the DTF design concept and how design variables are chosen to realize temporal encoded CDMA systems. Section 5 provides a complete analysis of the electronic SAE scheme that serves to underline the functionalities and design of the DTFs. Section 6 discusses analysis based on experimental results of DTF prototypes working at low speeds. Section 7 concludes the paper.

2. Spectral Amplitude Encoded System

The novel electronic system is motivated by precursory work on the field of Frequency-Encoded Optical CDMA by M. Kavehrad and D. Zaccarin [20]. The SAE technique was introduced as an advanced scheme that makes complete cancellation of MAI possible. Figure 1 illustrates the initially proposed scheme based on a bulk optical system with the capacity to create a fairly large number of orthogonal channels. The incoherent CDMA system allows the use of simple intensity direct-detection receivers and low cost non-coherent light sources, such as light-emitting diodes (LEDs). LEDs exhibit large spectral width and light pulses are not coherent and can provide the spectral requirement for high speed processing. Frequency components from ultra-short optical pulses are resolved by the encoders mask. The optical beam is coupled into the fiber link and, through a passive star coupler as that shown in Fig. 1, each transmitter can broadcast encoded data.

To select the corresponding transmitter address sequence, the receiver processes the incoming signal with a spectral amplitude filter, $A(w)$ as well as with a complementary filter, $\bar{A}(w)$. The variable w is the code weight. Since optical filtering obeys a positive function, the bipolar reception of non-coherent pulses is performed by the other part of the receiver, which comprises a balanced receiver that obtains the difference between the two photodetector outputs. Bipolar orthogonal codes can be implemented in the decoder. Unmatched transmitters will create a common disturbance on both branches of the receiver. Half of the frequency components match to the direct filter function and the other half match to the complementary one leading to a complete cancellation of interference. A matched user will produce an output pulse in correspondence to the code

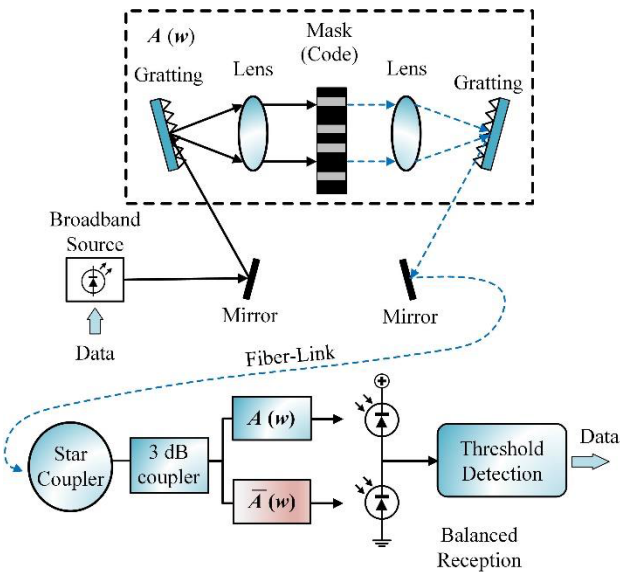

Fig. 1 Schematic of optical SAE-CDMA with balanced differential detection.

weight. Full orthogonality among users assumes frequency alignment between the frequency slots of encoded channels and the optical receiving filters.

The main objective of this work is to introduce new perspectives of the DTF method by exploring its analog code modulation characteristics, which have not been considered previously in CDMA systems. The proposal focuses on a SAE system and in our electronics approach code information is conveyed on spectral amplitudes of users. Encoders spread ultra-short pulses in time by forming a code modulated pattern programed in DTFs. On the other hand, decoders manipulate power of user subbands using square-law detection while dropping out user phases. The differential detection includes two DTFs intended to shift phases of input subbands. This scheme provides a basis to implement and test the transversal filter method.

3. DTF Topology

Figure 2 shows a conceptual schematic of the DTF. For accurate modelling of DTF, it is necessary to distinguish distributed circuit components that delay and amplify input pulses from components that shape ultra-short pulses. The inherent bandwidth limitation of all distributed active cells has to be accounted for in the model and included as a broadband frequency function. The overall pulse shaping function introduces a flat delay and low in-band distortion over the filter bandpass function. Therefore, an ideal narrow pulse applied to the Input (top left representation in Fig. 2) will result in a spread of output pulses of edges with slower rise than the original (bottom right representation in Fig. 2).

Analog circuit design strategies, previously considered for symbol-rate DTFs in [5], are applied for our proposed filter design. The synthesis of the filter follows the techniques used in CDMA ([5] and [6]). Tap gains are adjusted by applying external bias voltages to set the tap gain weight vector $\boldsymbol{g} = (g_1, g_2, \ldots, g_N)$; all normalized to the maximal gain which is set effectively by active devices (transconductance). Input pulses are delayed by cascading basic delay sections to set the vector $\boldsymbol{\tau} = (\tau_1, \tau_2, \ldots, \tau_N)$, thereby approximating to the required "analog" interstage delay. The impulse response of the N-tap DTF is given by (1) as:

$$h_{DTF}(t) = \sum_{n=1}^{N} G_n p\left(t - \sum_{k=1}^{n} \tau_k\right), \tag{1}$$

where $p(t)$ is the input pulse. Since the bandpass functions of transversal filters require both positive and negative tap gain coefficients, G_n denotes the *nth*-element of a vector of positive and negative amplitude-weighted coefficients.

In this study, we employ DTFs with predetermined FIRs that are chosen for their suitability for encoding and resulting in sequences with good correlation properties. The filter structures are not reconfigurable in terms of variable delay adjustment and thus code dictates their specific design. It is worth mentioning that DTF structures with the capacity to adjust tap gain weights and switch the sign of taps have been reported in the literature (for example in [9] and [10]), where distributed active stages are implemented as Gilbert cells providing balanced characteristics and broadband matching. However, the complexity at transistor-level design will be a key point to be taken into consideration in the selection of the filter topology. Figure 3 shows a schematic of the DTF employed in this work. The structure is termed the triple line structure, whose microwave characteristics were analyzed in [5] and [21] and is utilized here for the proof-of-concept in monolithic integrated circuit (MIC) form. Each active cell consists of two Heterojunction Field-Effect Transistors (HFETs) which are capacitively coupled to a common gate artificial transmission line (ATL). Unequal interstage delays are accomplished by adopting the reverse-gain filter topology, whereby the delay is set to be equal to the additive delay in gate and drain line sections. The input gate-ATL is shared by two rows of active devices and has pulse shaping characteristics. Ohmic losses in the gate junctions of active devices results in a reduced pulse dispersion and diminished high frequency oscillatory components.

DC bias circuitry (omitted in the schematic) allows tap gain control through the variation of the transistors' RF transcoductance. The tap gain control capability avoids disrupting the uniform impedance in ATLs. Each active cell couples actively common and differential signals that propagate simultaneously along drain lines. The passive balun component used shows low phase deviations across the filter

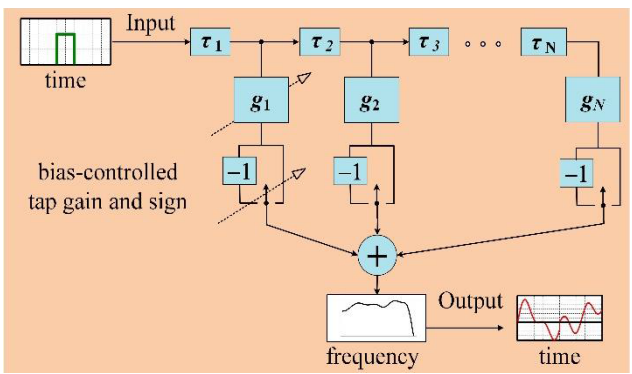

Fig. 2 Conceptual schematic of the FIR filter with unequal stage delays and unequal tap gains.

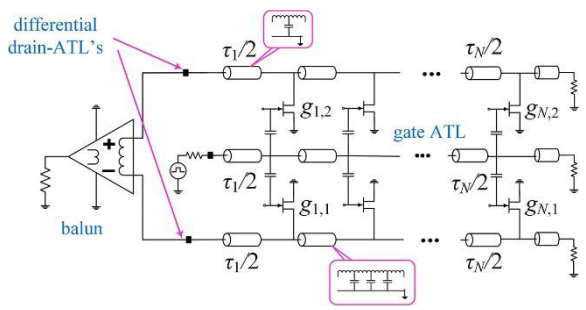

Fig. 3 Schematic of the traveling wave filter, where enclosed stages are required to achieve maximal and minimal delays.

bandwidth, resulting in diminished errors in the differential signals at the output port.

4. Design Concepts and Practical Implementations of DTFs for CDMA

Different filter structures have been considered for use in CDMA systems. For instance, prototype transversal equalizers with tap gain and sign control in [3] were applied with Gold codes to enable high-speed CDMA for optical access over PONs. This prototype equalizer is a practical (but limited) solution for electronic FIR transversal filter with non-return-to-zero modulation. However, given that the transversal equalizer has interstage delays shorter than the input pulse width, the output bit patterns suffered from substantial concatenation, particularly for late arriving pulses. On the other hand, a DTF has been designed with much larger delays between active cells with the aim of impressing codes on variable distance between unipolar pulses [6]. Such filter method is suitable for encoding and decoding with optical orthogonal codes (OOCs) [1]. Distributed circuits can be implemented to exhibit minimal inter-pulse interference in return-to-zero code modulated patterns.

Based on the flexibility with which the DTF can be designed, we propose a filter method that allows for a controlled level of interference between consecutive pulses as a variable to be included in new filter FIRs. Practical prototypes (such as those characterized by many degrees of freedom in their design) can provide pulse responses that conveniently approximate to phase-coded signals as in (2)

$$h(t) = w(t) \sum_{n=1}^{M} c_n \cos(\omega_n t - \beta_n), \tag{2}$$

where M is the number of the available subbands, $\omega_n = 2\pi n/T$, with T is set to be equal to the span time of the filter delay line, $w(t)$ is a time window with, $w(t) = 1$; for $0 < t < T$, and $w(t) = 0$; elsewhere. For brevity, the symbols c_n and β_n are referred to as the amplitude and phase of *nth*-subband, respectively. The designed waveform consists of M frequency slots, separated by $1/T$ Hz from neighboring frequency bin centers, therefore; T sets the frequency resolution of the coded patterns. The time window is a good approximation of practical filter responses.

The design depends on the selection of a number of taps that allows shaping the response by (2). The span time of the tapped delay line is a primary concern. DTF responses are affected by pulse broadening and attenuation introduced by delaying stages, which are constructed effectively as lightly damped linear-phase filters. A large number of such stages will result in significant pulse broadening. The practical design is based on the model shown in Sect. 2 (Fig. 2), whereby the overall filter 3-dB point can be chosen regardless of the selection of gain and delay parameters to implement a FIR function. If the behavior of broadband structures satisfies the frequency requirement of an elemental short input pulse, the DTF response becomes a linear combination of constituent pulses each showing similar transient parameters. This design property has been assessed for use in DS-CDMA systems [5] and, in this work, we use this property to extend the DTF method to spectrally encoded systems.

To generate a given CDMA signal, the amplitudes and phases of the subbands in (2) are set according to a specific code. Such a process is achieved through FIR filter synthesis, which is carried out by taking N sample points at the maxima and minima of the target function. To achieve frequency alignment between transmitter and receiver functions, the spectral content of all functions must exhibit the same frequency resolution. This leads to design all filters with the same span time.

The inverse Fourier transform of each frequency function (shaped by code) becomes a target function, which is approximated by a filter synthesis implementing DTFs with a variable number of taps. The number of taps is set to equal the number of samples and their amplitudes and time positions determine the gain values and interstage delays of the filter elements shown in Fig. 2. We use Hadamard codes in Table 1 (Sect. 5.2) and choose to set the amplitude of coded subbands at the highest frequency to a 'one' code element. We found that the synthesis employing FIR functions conveying code information in 5 subbands results in viable design requirements. The FIRs can be approximated by DTFs with 6, 7 or 8 taps, depending on code. Accordingly, all CDMA sequences will show a fast changing component, which results in the same bandwidth requirement for all filter designs. Similarly, the construction of receiver and receive functions with elemental pulses of duration equal to $T/N_{\max}$, with $N_{\max}$ being the maximal number of taps (equal to 8) satisfies time and frequency requirements to approximate a CDMA sequence.

Experimental results are based on transversal filters implemented in MIC form. The 3-dB point was set at 1 GHz and the input pulse width equal to 1 ns. Since $N_{\max} = 8$, the span time of all filters was set to be equal to 8 ns thereby providing the same frequency resolution (1/8 ns = 125 MHz) in all filter responses.

In this work, an algorithm, based on detailed circuit models, is developed to optimize the magnitude response. This is achieved by applying tap gain variation and delay around the nominal values derived in the filter synthesis step. Figure 4 displays measured results of a 6-tap prototype and the reference (target) signal that depends on the amplitude and phase vectors $\boldsymbol{c} = (0, 1, 1, 1, 1)$ and $\boldsymbol{\beta} = (0, -\pi/2, \pi, \pi/2, 0)$, respectively. Note that harmonically related sinusoids in (2) can be well approximated by the filter pulse response. Although good temporal match is apparent, the large attenuation introduced by microwave devices, which is compensated by tap gain adjustment, limits the filter's tunability.

DTFs constructed with unequal differential stage delays will present concatenation between subsequent pulses in a pattern. To illustrate this effect, Fig. 5 displays independent tap responses of the implementation. It is seen that

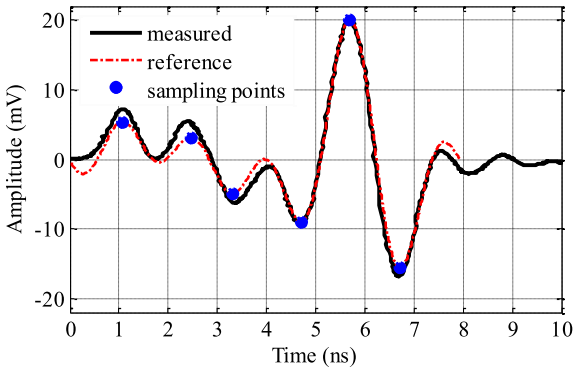

Fig. 4 Measured FIR of the 6-tap DTF prototype.

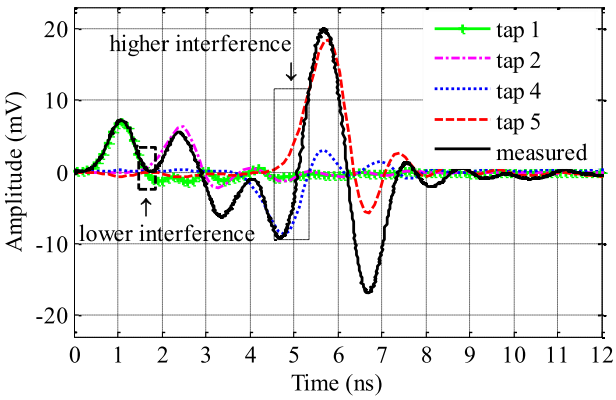

Fig. 5 Individual DTF tap responses introducing minimal and maximal interpulse interference.

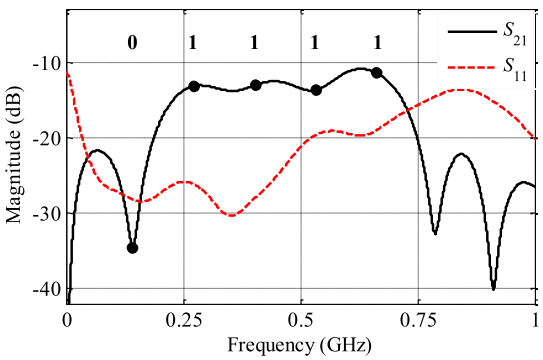

Fig. 6 Simulated parameters of the DTF prototype and balun component.

larger stage delay between Tap 1 and Tap 2 creates low interference in the pattern, whereas by allowing for an amount of interference between Tap 4 and Tap 5 responses, the summation of both channels results in a good approximation about the sampling point. Individual tap responses shape smooth pulse transitions and provide good match with target functions. At this regard, the shaped analog waveforms compare favorably with conventional SS chip shape formats since the DTF is unable to change to binary states rapidly.

Figure 6 displays the frequency responses of the filter. The frequency gain transmission $|S_{21}|$ becomes a bandpass

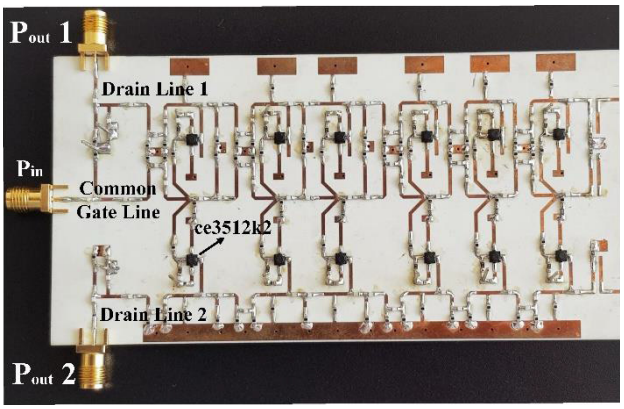

Fig. 7 Prototype of a 6-stage DTF circuit in SMD technology.

function aimed at shaping input subbands separated by 125 MHz from neighborhood subbands. The DTF output has a spectrum shaped by the implemented code. The parameter $|S_{21}|$ is formed by subbands and interfering side lobes that spread over the available bandwidth. The amplitude of the first subband, which corresponds to a 'zero' code element, results to be 21.8-dB (in average) smaller than the other subbands' amplitudes modulated by a 'one' code element.

The low frequency gain over the bandwidth ($|S_{21}| < -10$ dB) results from the large attenuation introduced by the microwave components employed. In addition, the discrete transistors used in the prototypes present a reduced gain (maximal transcondance of 149 mS and intrinsic voltage gain of 14.9). Figure 6 also displays the reflection parameter, which is at an acceptable level of being better than -10 dB across the band.

As shown in a following section, the 6-tap DTF is intended to shift subband phases by the phase code $(0, -\pi/2, \pi, \pi/2, 0)$. As a proof-of-concept, we fabricated a prototype using commercial off-the-shelf GaAs discrete FET transistors ce3512k2. Figure 7 shows the constructed prototype based on the design method. A manageable number of delay stages are obtained by setting the 3-dB point to a half of the (Bragg) cut-off frequency of ATLs. Thin film inductors and capacitors in the form of surface mount devices (SMDs) allows setting the filter cut-off frequencies with reasonable accuracy. An additive capacitance in shunt with active cells (not shown in the schematic in Fig. 3) allows keeping a uniform stage capacitance (C). ATLs are designed with the same characteristic impedance $Z_0 = \sqrt{L/C}$, where L is the inductance per section. Drain signals travel with practically the same delay characteristics; each basic delay section in introduces delay equal to $Z_0 C$ (= 0.23 ns) and their cascade arrangement allow sets the analog delay. A 50-Ohm system is employed to facilitate testing of the structures.

5. Electronic SAE-CDMA

5.1 Correlation

In previous demonstrations of ECDMA, DTFs achieve DS temporal encoding functions and the correlators perform despreading functions for matched and unmatched users. In such systems, the large levels of MAI limit performance. Our proposal is for a technique compatible with the capabilities of DTFs by which user interference can be effectively diminished. The structures illustrated in Fig. 8 provide an approximation to spectral encoding/decoding and have been proposed for spread time (ST)-CDMA. The "spectral" decoder can be implemented by a correlator programed with a spread-in-time signal truncated by a time window. The decoder outputs a detection pulse at the sampling time if the initial phases of user subbands match the "conjugate" phases of the decoder. Although correlative interference can be made equal to zero by code, large side lobes appearing at the output reduce the rejection of additive interference and therefore may compromise overall performance when a threshold scheme is included in a subsequent data recovering stage.

Instead of performing matching filtering as implemented in DS and ST-CDMA systems, the correlation method is intended to modify the amplitudes and phases of input subbands. In the electronic SAE approach, the correlator output remains spectrally spread for all users. The response of a correlator with FIR function that depends on amplitudes $(d_1, \ldots, d_M)$ and phases $(\varphi_1, \ldots, \varphi_M)$ to the user given by (2) is shown in (3)

$$z(t) = \frac{1}{2}\sum_{n=1}^{M} c_n d_n r(t)\cos(\omega_n t + \varphi_n - \beta_n), \tag{3}$$

where the function $r(t)$ is the autocorrelation of $w(t)$ and $z(t)$ is the periodic correlation between the impulse responses of the encoder/decoder; $h_e(t)$ and $h_d(t)$, respectively. This correlation function describes frequency alignment between main lobes of encoder and correlator functions. In the following, (3) is shown to allow the description of a spectral encoded system that achieves full orthogonality. The aperiodic correlation of truncated spread-in-time signals necessarily includes frequency overlapping [18] and its effects are assessed in the experiments.

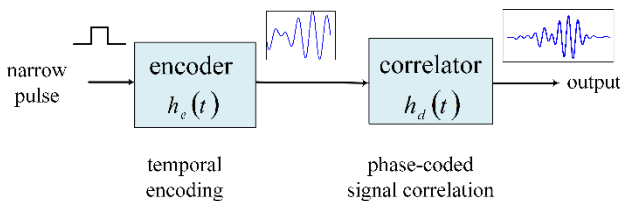

Fig. 8 Transversal encoder and correlation structures.

5.2 SAE System

An SAE-CDMA system scheme illustrating an encoder-decoder pair is shown in Fig. 9. The transmitted spectra is a set of harmonically related signals modulated in amplitude by a data pulse. On the other hand, the decoder comprises two DTFs acting as correlators. Input power is split into two receiver branches each forming an encoder/correlator pair. At the upper arm, the initial phases of the correlation function correspond to a unique code that provides the address of a specific node receiver. The lower arm shifts the phases of user subbands by $(\theta_1, \ldots, \theta_M)$. This FIR function has a unit amplitude vector to set a common reference signal to demodulate correlated users. Notice that the mixer output is effectively the correlation between the spectra of both correlator outputs, however, only the correlation product of frequency-aligned signals gives rise to a mixing product around dc. The subband demodulation is a synchronous process given the existing time alignment of the address correlation signal $z_\varphi(t)$ to the reference signal $z_\theta(t)$.

After lowpass filtering, the decoder output Z will be as shown in (4).

$$Z = \int_0^{2T} z_\varphi(t) z_\theta(t) dt \tag{4}$$

Assuming normalized power values, so the energy of the decoded pulses (ε) is the same for all users and after substituting the corresponding amplitude and phase vectors (as

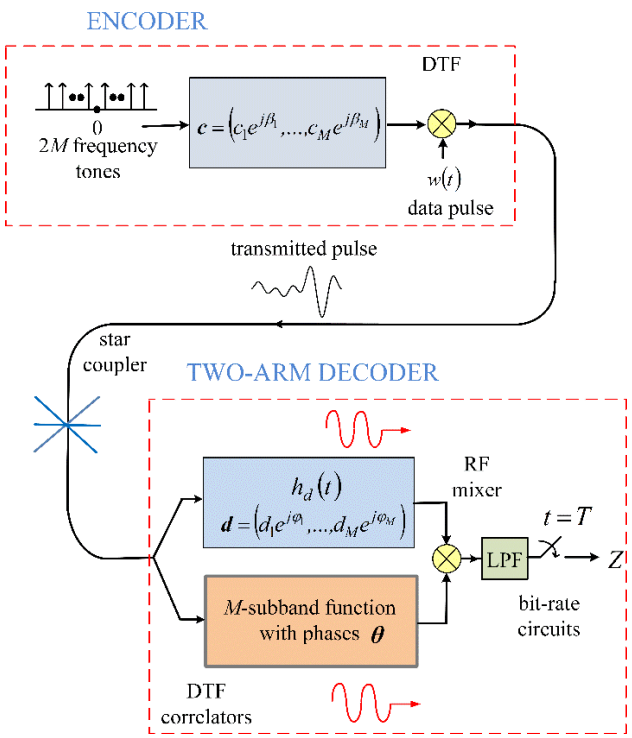

Fig. 9 Electronic SAE-CDMA, where the amplitudes and phases of DTF functions are shown in the positive half of the spectrum.

Table 1 Hadamard codes of length 4, unipolar and phase mapping.

Hadamard code	Unipolar code	Code phase φ referred to θ
(1, 1, 1, 1)	(1, 1, 1, 1)	($\pi/2$, 0, $\pi/2$, 0)
(−1, −1, 1, 1)	(0, 0, 1, 1)	($-\pi/2$, π, $\pi/2$, 0)
(1, −1, −1, 1)	(1, 0, 0, 1)	($\pi/2$, π, $-\pi/2$, 0)
(−1, 1, −1, 1)	(0, 1, 0, 1)	($-\pi/2$, 0, $-\pi/2$, 0)

indicated in Fig. 9), one arrives at (5)

$$Z = \varepsilon \sum_{n=1}^{M} c_n^2 d_n \cos(\varphi_n - \theta_n). \tag{5}$$

Accordingly, the computed dc component will depend on the square rise of user subband amplitudes (c's, see Fig. 9) whereas the phases are lost after demodulation. The DTFs at the decoder shift the phases of input subbands to set a reference to add detected subbands in phase or anti-phase. Ideally, bipolar decoding could accomplish perfect orthogonality among users.

Unipolar-bipolar code constructions proposed in [20] is utilized for processing temporal phase-coded signals. Table 1 lists orthogonal Hadamard codes of length 4 and the code mapping of amplitudes and phases to achieve bipolar detection. Coding is effected by imposing unipolar code elements on the amplitudes of spectral subbands. In the other column, phases are set by mapping bipolar codes on a unit circle. From (5) bipolar decoding requires taking phase differences $\varphi_n - \theta_n$ on 0 and π for all the M subbands. Code phase vectors itemized in Table 1 are shifted by the alternate reference vector $\boldsymbol{\theta} = (\pi/2, 0, \pi/2, 0)$. A set of phases uniformly spaced on the unit circle 0, $\pm\pi/2$ and π becomes the address of a given decoder.

The alternate vector $(\pi/2, 0, \pi/2, 0, \ldots)$ is one of the possible sets of reference phases that could be used in the decoder. This selection however plays an important role in the performance of the decoder. The appearance of interfering side lobes in the correlation functions performed by filter structures (as described in Sect. 4) creates potential interference, particularly after mixing the address correlation signal with the reference by the decoding process of Fig. 9. It has been proven, via simulation of MMICs that the phases in Table 1 can lead to a consistent improvement in the decoding for all CDMA signals [18]. In the following experiments, it is shown that the resulting complexity of the created analog pulse patterns attaining the potential advantages of the SAE systems.

6. Results

To test the capabilities of the scheme, encoder/correlator structures were analyzed experimentally. DTFs were implemented as MIC prototypes working at low speed (1-GHz cut-off frequency and 8-ns span time). All FIRs have the first subband set to a zero code element to diminish side lobe interference near dc.

Some FIRs that depends on the coded phase elements

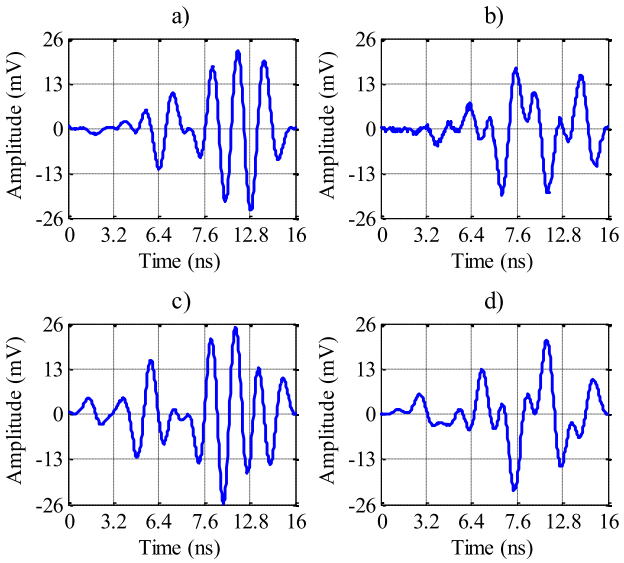

Fig. 10 Measured correlations of the decoder $(0, -\pi/2, \pi, \pi/2, 0)$. Responses at the upper arm (address) to user a), and interferer b); and responses at the lower arm (reference) to user c) and interferer d).

listed in Table 1 present discontinuities at both edges of the time window. The discontinuities at 0 and T are incompatible with the rise time constraints of the DTF. To make the synthesis workable, we notice that the decoder scheme has a degree of freedom in the selection of phases. This is established by noticing that a constant phase shift applied to both decoder's functions results in the same output, as shown in (5). Computer analysis indicates that most of the FIR functions do not present discontinuity when a phase of +1.1 radians is added to all phase elements. This is the case of the FIR function shown in Fig. 4, which will be used in the decoder with address $(0, -\pi/2, \pi, \pi/2, 0)$.

Figure 10 displays measured results of DTFs in back-to-back configuration. The user code (0, 0, 0, 1, 1) and interferer code (0, 1, 0, 0, 1) were correlated with the address (at the upper arm) and with the reference (at the lower arm) of the decoder.

In these experiments, the correlation relies on the ability of encoder/correlator DTFs to keep the duration of elemental pulses, δ_T, to the ratio $T/N_{\max}$, (as stated in Sect. 4). Those basic pulses are shaped by damped linear filters constituting ATLs. The correlation patterns in Fig. 10 have a fast changing component of a rate equal to $(2\delta_T)^{-1}$, which sets the maximal frequency of the correlation between phase-coded signals, f_{M} $(= \omega_{\mathrm{M}}/2\pi) = 1/2\delta_T$. Since travelling pulses are nearly symmetrical and exhibit a rise time (τ_r) approximately equal to the fall time (τ_f) then $\delta_T = \tau_r + \tau_f \cong 2\tau_r$. Taking into account the overall rise time-bandwidth product of the DTF ($\tau_r \times f_{3\mathrm{dB}} \cong 0.35$), the maximal subband frequency, that can be synthesized, depends ultimately on the filters' cut-off frequency. From the above, one can confirm that the 3-dB point of the DTFs must be at least equal to $1.4 f_{\mathrm{M}}$ (= 875 MHz), which is satisfied in our implementations.

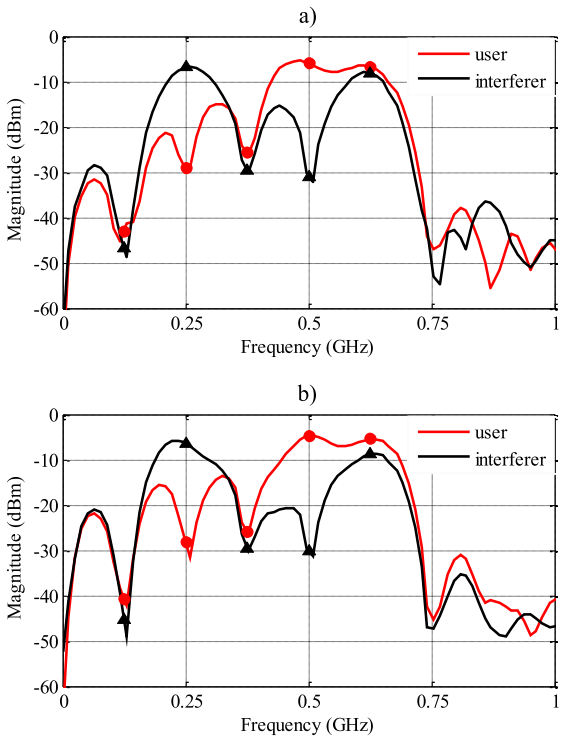

Fig. 11 FFT of the correlations shown in Fig. 10, a) upper arm (address) responses and b) lower arm (reference) responses.

Figure 11 shows the FFT of the measured correlations using a 5-GHz sampling oscilloscope. The responses correspond to spectrally shaped signals at discrete frequencies (indicated by markers). The results from both user and interferer codes are similar in both branches of the decoder. The 'zero' code element has a spectral amplitude of 21.4 dB lower than the amplitudes of 'one' elements' (on average). Notwithstanding, higher side lobes around 'zero' code frequencies are apparent.

The amplitudes of interfering components at discrete frequencies depend on how accurate DTF responses can approximate spread-in-time signals given by (2) as well as by the sidelobes created by correlation. The side-lobe components will generate interference at the output of the decoder in Fig. 9. It is worth mentioning that a quantitative analysis of signal-to-interference ratio depends on the amplitudes and phases of the correlators' responses [18]. As such, the spectral amplitudes shown in Fig. 11 do not suffice to set targets for the code-based multiplexing function.

The despreading operation involves the demodulation of the correlated spectra followed by a lowpass filter (LPF) (see Fig. 9). Each subband is detected by square-law detection and manipulated separately by differential decoding. Figure 12 shows simulation results of the demodulation using the measured waveforms. Code matching and interference rejection are plotted over the same time scales for comparison purposes. The figure displays temporal responses of the mixer output when a user code $(0, 0, 0, 1, 1)$ is matched to the receiver phase code $(0, -\pi/2, \pi, \pi/2, 0)$. Code matching results fundamentally in a unipolar signal, which corresponds to the detection of energy of input subbands.

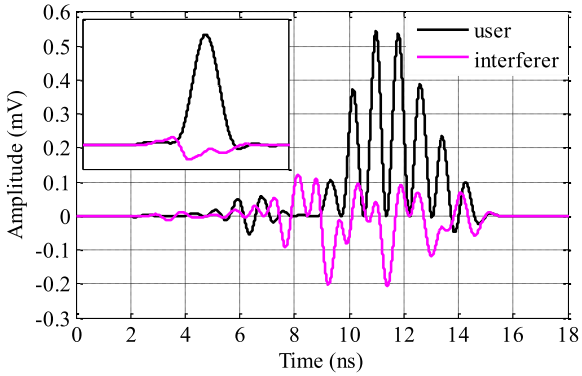

Fig. 12 Simulation results of the receiver with address $(0, -\pi/2, \pi, \pi/2, 0)$, user $(0, 0, 0, 1, 1)$ and interferer $(0, 1, 0, 0, 1)$. Mixer output and (inset) after LPF.

Contrariwise, a user with code $(0, 1, 0, 0, 1)$ will create interference, on average, close to zero. The inset displays the mixer output passing through a LPF, which is a 4^{th}-order Butterworth of cut-off frequency equal to 0.1 GHz. The amplitude of the output pulse is proportional to the power of two successfully decoded subbands whereas the interferer is decoded by adding detected subbands inphase and antiphase to cancel out user interference. Comparison between both filter responses indicates good interference rejection margins over the complete decoding time. Results confirm that the decoder output is linked to frequency aligned main lobes of encoder/correlator subbands and to a lower extent to subband interference.

7. Conclusions

A DTF method for ECDMA system was investigated. A DTF model by which bandwidth limiting effects are distinguished from delay and gain circuit components was considered for design. Measurements of prototypes in MIC form prove the design concept and circuit functionalities. Temporal phase-coded signals can be approximated by multilevel pulse patterns that present controlled levels of interpulse interference, which permits an extension of the filter method. An electronic SAE scheme that employs square law detection of user subbands forms the basis to design and test our filter method. It is shown that the potential benefits of the SAE scheme may be realized, provided that the DTF method allows the maximal degree of freedom in the design.

The design method investigated in this paper may be taken as a foundation for future developments of SAE-CDMA systems at higher speeds. Different factors affecting accuracy and associated with circuit non-idealities need to be considered for multi-Gbit/s system implementations. An advantage that makes this approach followed attractive is in its allowance of the detection of user data with circuits working at the operating bit-rate (instead of working at the higher chip-rate, as required in DS-CDMA systems). This simplifies the practical receiver design and allows the imple-

mentation of high speed system using affordable technologies.

References

[1] J.A. Salehi, "Code division multiple-access techniques in optical fiber networks. I. Fundamental principles," IEEE Trans. Commun., vol.37, no.8, pp.824–833, Aug. 1989. DOI:10.1109/26.31181.

[2] K. Kitayama, Optical Code Division Multiple Access: A Practical Perspective, Cambridge University Press, Cambridge, UK, 2014.

[3] J.B. Rosas-Fernandez, J.D. Ingham, R.V. Penty, and I.H. White, "18 Gchip/s electronic CDMA for low-cost optical access networks," J. Lightwave Technol., vol.27, no.3, pp.306–313, Feb. 2009. DOI:10.1109/JLT.2008.2010414.

[4] J. Aguilar-Torrentera and I. Darwazeh, "A distributed-based transversal filter for Gbit/s spread-spectrum systems," Proc. International Conference on Telecommunications, vol.1, pp.1248–1252, Beijing China, 2002.

[5] J. Aguilar-Torrentera and I. Darwazeh, "Dual drain-line distributed cell design for multi-Gb/s transversal filter implementations," Proc. 2005 International Symposium on Circuits and Systems, pp.3958–3961, Kobe, Japan, 2005. DOI:10.1109/ISCAS.2005.1465497.

[6] M. Pimenta and I. Darwazeh, "Circuit design proposal for multi-GBit/s CDMA over fibre using distributed topologies," Proc. 9th International Symposium on Communications and Information Technology, pp.1000–1005, Incheon, Korea, 2009. DOI:10.1109/ISCIT.2009.5340997.

[7] G.C. Gupta, M. Kashima, H. Iwamura, H. Tamai, T. Ushikubo, and T. Kamijoh, "A simple one-system solution COF-PON for metro/access networks," J. Lightwave Technol., vol.25, no.1, pp.193–200, Jan. 2007. DOI:10,1109/JLT.2006.887187.

[8] J.B. Rosas-Fernandez, J.D. Ingham, R.V. Penty, and I.H. White, "18 Gchip/s error-free OCDMA transmission with electronic processing for PON applications," Proc. 34th Conference on Optical Communication, pp.1–2, Brussels, Belgium, 2008. DOI:10.1109/ECOC.2008.4729545.

[9] H. Wu, J.A. Tierno, P. Pepeljugoski, J. Schaub, S. Gowda, J.A. Kash, and A. Hajimiri, "Integrated transversal equalizers in high-speed fiber-optic systems," IEEE J. Solid-State Circuits, vol.38, no.12, pp.2131–2137, Dec. 2003. DOI:10.1109/JSSC.2003.819084.

[10] C. Pelard, E. Gebara, A.J. Kim, M.G. Vrazel, F. Bien, Y. Hur, M. Maeng, S. Chandramouli, C. Chun, S. Bajekal, S.E. Ralph, B. Schmukler, V.M. Hietala, and J. Laskar, "Realization of multigigabit channel equalization and crosstalk cancellation integrated circuits," IEEE J. Solid-State Circuits, vol.39, no.10, pp.1659–1670, Oct. 2004. DOI:10.1109/JSSC.2004.833569.

[11] M. Pimenta and I. Darwazeh, "Experimental demonstration of electronic GVD compensation in optical CDMA networks," Proc. Summer Topical Meeting, LEOSST '09, IEEE/LEOS, pp.25–26, Newport Beach, CA, USA, 2009. DOI:10.1109/LEOSST.2009.5226238.

[12] A. Borjak, P.P. Montero, J. O'Reilly, and I. Darwazeh, "High-speed generalized distributed-amplifier-based transversal-filter topology for optical communication systems," IEEE Trans. Microw. Theory Techn., vol.45, no.8, pp.1453–1457, Aug. 1997, DOI:10.1109/22.618451.

[13] P. Montero, A. Borjak, J.F. da Rocha, J. O'Reilly, and I. Darwazeh, "Adjustable post-detection filters for optical amplified soliton systems," IEICE Trans. Electron., vol.E85-C, no.3, pp.511–518, 2002.

[14] A. Al-Dabbagh, T. O'Farrell, and M. Darnell, "Optical signal design using reciprocal sequences," Electron. Lett., vol.34, no.20, pp.1962–1964, Oct. 1998. DOI:10.1049/el:19981375.

[15] S. Pavan and S. Shivappa, "Nonidealities in traveling wave and transversal FIR filters operating at microwave frequencies," IEEE Trans. Circuits Syst. I: Regular Papers, vol.53, no.1, pp.177–192, Jan. 2006. DOI:10.1109/TCSI.2005.854610.

[16] J.B. Rosas-Fernandez, J.D. Ingham, R.V. Penty, and I.H. White, "Scalability techniques in electronically processed CDMA for low cost and flexible optical access networks," Proc. 11th International Conference on Transparent Optical Networks, Islas Azores, Portugal, 2009. DOI:10.1109/ICTON.2009.5185304.

[17] X. Guo, Q. Wang, X. Li, L. Zhou, L. Fang, A. Wonfor, J.L. Wei, J. von Lindeiner, R.V. Penty, and I.H. White, "First demonstration of OFDM ECDMA for low cost optical access networks," Optics Letters, vol.40, no.10, pp.2353–2356, May 2015. DOI:10.1364/OL.40.002353.

[18] J. Aguilar-Torrentera, J.R. Rodríguez-Cruz, N.P. Puente-Ramírez, and G. Rodríguez-Morales, "Spectral-amplitude encoding CDMA system based on high-speed electronic encoder/decoder structures," Rev. Fac. Univ. Antioquia, vol.78, pp.99–104, 2016. DOI:10.17533/udea.redin.n78a13.

[19] P.M. Crespo, M.L. Honig, and J.A. Salehi, "Spread-time code-division multiple access," IEEE Trans. Commun., vol.43, no.6, pp.2139–2148, June 1995. DOI:10.1109/26.387455.

[20] M. Kavehrad and D. Zaccarin, "Optical code-division-multiplexed systems based on spectral encoding of noncoherent sources," J. Lightwave Technol., vol.13, no.3, pp.534–545, April 1995. DOI:10.1109/50.372451.

[21] J. Aguilar-Torrentera and I. Darwazeh, "Performance analysis of a monolithic integrated transversal filter using mixed-mode scattering parameters," IET Microwave, Antennas and Propagation, vol.1, no.4, pp.925–931, Aug. 2007. DOI:10.1049/iet-map:20060181.

Jorge Aguilar-Torrentera received the M.S. degree from Research and Advances Studies Center (CINVESTAV) campus Mexico City in 1998. He obtained a Ph.D. degree from University College London (UCL) in 2004 in the field of OCDMA. During 2004–2009, he stayed at Intel Labs, where he was engaged in research on RF systems and high-speed interconnects. From 2014, he is a full-time professor at Universidad Autónoma de Nuevo León, México.

Gerardo García-Sánchez received the degree of Engineer of Electronics and Communications from Faculty of Mechanical and Electrical Engineering at Universidad Autónoma de Nuevo León during the period 2008–2013. He worked in Avaya Communications of Mexico during the period 2013 – ending in 2014. Currently, he is a student of Master of Science in Electrical Engineering, in Telecommunications.

Ramón Rodríguez-Cruz received the M.S. degree from University of Texas at Arlington in 1995 and he obtained a Ph.D. degree from Research and Advances Studies Center (CINVESTAV) in 2000. During 2001–2011, he was a full-time professor at ITESM campus Mty. From 2011, he is a full-time professor at Universidad Autónoma de Nuevo León, México.

Izzat Z. Darwazeh received the Graduate degree in electrical engineering from the University of Jordan, Amman, Jordan, in 1984 and the M.Sc. and Ph.D. degrees from the University of Manchester, In the U.K., in 1986 and 1991, respectively. He currently holds the University of London Chair of Communications Engineering and leads the 70-strong Communications and Information Systems Group, Department of Electronic and Electrical Engineering, University College London, London, U.K. He has authored or coauthored more than 250 papers in the areas of optical and wireless communications and monolithic microwave integrated circuits and high-speed/frequency circuits. He coedited Analogue Optical Fibre Communications (IEE, 1995) and was a coeditor of the 2008 Elsevier-Newness book on electrical engineering. He is also the coauthor of two books on Linear Circuit Analysis and Modelling (Elsevier, 2005) and on Microwave Active Circuit Analysis and Design (Academic Press, 2016). He currently teaches mobile and wireless communications and circuit design, and his current research activities include ultrahigh-speed microwave circuits and wireless and optical communication systems. In 1993 he proposed with Paulo Moreira and John O'Reilly the use of distributed amplifiers for processing and shaping of multi Gbit/s optical signals and in 2015 he collaborated with Professor Ziraths group at Chalmers university to design the worlds widest band amplifier (near DC to 235 GHz). Prof. Darwazeh is the Director of UCL Institute of Communications and Connected Systems (UCL-ICCS). He is a Chartered Engineer, a Fellow of the IET, and a Fellow of the Institute of Telecommunications Professionals (FITP).